

© 2021. Meng Liu, Quansheng Sun, Haitao Yu, Jianxi Yang, Tongzhou Zhang.

pp. 369–381

This is an open-access article distributed under the terms of the Creative Commons Attribution-NonCommercial-NoDerivatives License (CC BY-NC-ND 4.0, <https://creativecommons.org/licenses/by-nc-nd/4.0/>), which permits use, distribution, and reproduction in any medium, provided that the Article is properly cited, the use is non-commercial, and no modifications or adaptations are made.



## Research paper

# Static and dynamic test analysis of a 12-years old 14 000-ton cable-stayed bridge used swivel construction technology

Meng Liu<sup>1</sup>, Quansheng Sun<sup>2</sup>, Haitao Yu<sup>3</sup>, Jianxi Yang<sup>4</sup>,  
Tongzhou Zhang<sup>5,6</sup>

**Abstract:** In order to study the change in performance of the Suifenhe cable-stayed bridge in China over 12 years, cable force, elevation, static and dynamic load tests were conducted in 2006 and 2018, respectively. In this paper, theoretical data, obtained through finite element model analysis, were compared with the measured load test data for changes in static and dynamic performances. A comparison between 2006 and 2018 shows that additional dead load deflection exists in the main span after 12 years of operation. And that the cable force due to dead load of the full-scale cable-stayed bridge decreases and redistributes, which have adverse effects on the safety of bridge structure after long-term operations. Therefore, on-site inspection, static and dynamic load tests are recommended for cable-stayed bridges over 10-years old to test their static and dynamic performance. Moreover, cable force adjustments are to be conducted whenever necessary for the cable-stayed bridge used swivel construction.

**Keywords:** cable-stayed bridge, cable test, swiveled construction, static and dynamic test

<sup>1</sup>School of Civil Engineering, Northeast Forestry University, 150040 Harbin, China, e-mail: [liumeng@nefu.edu.cn](mailto:liumeng@nefu.edu.cn), ORCID: 0000-0001-8438-3755

<sup>2</sup>Prof., PhD., Eng., School of Civil Engineering, Northeast Forestry University, 150040 Harbin, China, e-mail: [sun-quansheng@nefu.edu.cn](mailto:sun-quansheng@nefu.edu.cn), ORCID: 0000-0002-7772-3499

<sup>3</sup>School of Civil Engineering, Northeast Forestry University, 150040 Harbin, China, e-mail: [871256175@qq.com](mailto:871256175@qq.com), ORCID: 0000-0002-4092-2005

<sup>4</sup>PhD., School of Civil Engineering, Northeast Forestry University, 150040 Harbin, China, e-mail: [yangjianxi@nefu.edu.cn](mailto:yangjianxi@nefu.edu.cn), ORCID: 0000-0002-9860-3410

<sup>5</sup>MSc., School of Civil Engineering, Northeast Forestry University, 150040 Harbin, China, e-mail: [tongzhou321@126.com](mailto:tongzhou321@126.com), ORCID: 0000-0001-7661-6141

<sup>6</sup>MSc., Yantai City Transportation Law Enforcement and Supervision Detachment, 264000 Yantai, e-mail: [tongzhou321@126.com](mailto:tongzhou321@126.com), ORCID: 0000-0001-7661-6141

## 1. Introduction

With their unique advantages of being prefabricated bridge structures located in a favourable position and then installed in place successfully, cable-stayed bridges solve major technical problems encountered by the traditional construction method during the construction process, equipment integration, intelligent monitoring and evaluation. Moreover, these bridges realise assembly construction across busy traffic lines in cities and canyons in mountain areas and thus have significant promotion value.

The level swivel of cable-stayed bridges in China started with the ZengDa Bridge with a swivel mass of 1,344 tons [1]. Wang Wuqin [2] introduced the swivel construction plan of a rigid cable-stayed bridge in Daliying Railway and explained that the spherical hinge is one of the key parts to guarantee the success of swivel. Mao Suoming [3] explored the construction procedure by using the swivel cable-stayed bridge along Shijiazhuang Ring Road. With their precise calculation and the rationality of on-site construction, key techniques have passed actual tests. Valuable experiences have been accumulated in relation to the swivel construction of cable-stayed bridges. Guo Yajuan et al [4]. Analysed the mechanical properties of the turntable of the Zoucheng cable-stayed bridge by establishing an ansys 3d finite element model. They proposed several methods, such as adding reinforcements, adjusting the slot size and wrapping the steel plate around the turntable to guarantee the smooth construction of the cable-stayed bridge swivel against uneven stress. Nui Yuanzhi [5] performed a comparative analysis of the type of swivel hinge of a single-tower space four-cable plane prestressed-concrete cable-stayed bridge. The analysis shows that the comprehensive performance of the spherical hinge is better than that of the flat hinge. Hu Jiehui [6] studied the deformation and stress state of an asymmetric single-tower cable-stayed bridge. The bridge structure has adequate strength and rigidity under the combination of dead load and unfavourable live load. Fuchs et al [7]. Explained the design and construction of the El Ferdan Bridge in detail and analysed the mechanical performance of the swivel system. Lv Liang et al [8]. and Cao Shaohui et al [9]. Conducted a load test and a finite element model calculation of the Lijiang River Extra-Large Bridge, a twin-tower partial cable-stayed bridge, and the Malinghe Extra-Large Bridge, a twin-tower cable-stayed bridge, to verify whether these bridges are in an elastic working state under test load. The actual bearing capacity of the bridges meets design requirements.

The level-pivot hinged swivel of cable-stayed bridges is mainly characterised by a high-precision butt joint of main and approach bridges; an innovative design; a large rotation radius; stable, safe and convenient processing, transportation and installation; and low cost. Scholars have paid considerable attention to research on the mechanical performance of cable-stayed bridges during bridge construction, and local research has been conducted on the pivoting components of the cable-stayed bridges in the horizontal pivoting process. Few researchers analysed the mechanical performance of level-pivot hinged cable-stayed bridges after the completion and operation of the bridges. The load test can directly measure the relevant parameters from theoretical analysis and calculation, explore the mechanical behaviour of the bridge structure, enrich and develop bridge calculation theory and verify the compatibility of a finite element model and a real bridge [10]. The present paper uses the Suifenhe cable-stayed bridge as the object of study and evaluates its bearing capacity and health status. On the basis of the load test data from the bridge completion in 2006 and the operation in 2018, we analyse the mechanical char-

acteristics of the level-swivel cable-stayed bridge combined with the finite element model. The analysis provides reliable technical data for its continued safe use, maintenance, reinforcement, reconstruction and load limiting.

## 2. Background

The swivel cable-stayed bridge studied in this paper is the Suifenhe cable-stayed bridge. Firstly, the foundation of the bridge tower is constructed west of the railway station, with the swivel temporarily fixed by a level-pivot hinge. Then, the support is established along the railway track, which is for cast-in-place of the main tower, piers and cantilever beam of the cable-stayed bridge. A swivel structure is formed from the tower, piers, beam and stay cables. Turntable-coordinated traction equipment composed of a hinge and a slide way with a small friction coefficient is used to rotate the whole bridge in place. The bridge has a total weight of 14 000 t, its span combination is 100 m + 100 m. The bridge surface is 23.5 m wide. Both the main girder and the main tower are constructed of C50 concrete. The prestressed steel strand with  $\Phi 15.20$  high strength and low relaxation is adopted. Staying cable adopts single cable surface fan-shaped arrangement. The standard strength of steel strand is 1860 MPa, and the specifications are 15–31, 15–34, 15–43, 15–55, 15–61. Its successful swivel has a wide range of social benefits and promotion value. The turntable and swivel are shown in Figs. 1 and 2.



Fig. 1. Location and installation of vinyl plate



Fig. 2. Support dismantling and swivel of the beam

Spatial finite element model construction for the cable-stayed bridge: The nodes are divided in accordance with the general rules of finite element division. On the basis of the actual condition of the main girder pouring of the bridge, we number the bridge from the main girder. The girder units are numbered 1 to 82. The tower is divided into 21 units, numbered 82 to 103. Cables B1 to B18 are numbered 104 to 121, and cables Z1 to Z18 are numbered 122 to 139. The beam188 girder unit is adopted in the main girder and the tower, and link10 is used in the cables.

Boundary condition: The displacement and rotation angle are constrained in three directions (longitudinal, horizontal and in the same direction of movement) of the main tower-bearing platform. In other piers, only longitudinal and horizontal directions are constrained, without considering the influence of support and expansion joint on the longitudinal restraint of the girder and the lateral rigidity of side piers. The Elevation drawing of the cable-stayed bridge and the FEM of the cable-stayed bridge are shown in Figs. 3 and 4, respectively.

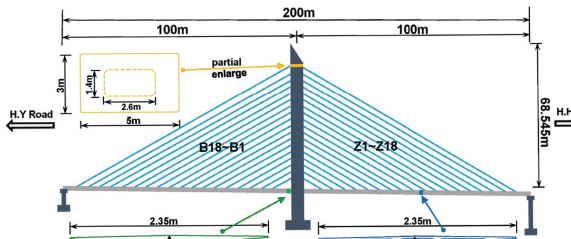


Fig. 3. Elevation drawing of the cable-stayed bridge

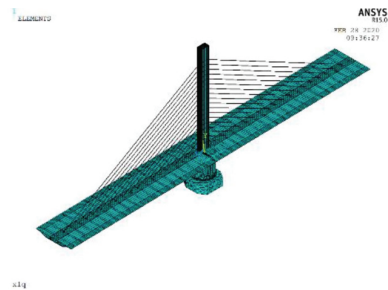


Fig. 4. FEM of the cable-stayed bridge

### 3. Dead load test of the cable force and elevation of the bridge floor

#### 3.1. Dead load test of cable force

The stay cable force is measured via the vibration frequency method [11, 12]. The test system for the cable force is shown in Fig. 5. The main frequency of the cable is obtained through frequency analysis. The cable force is obtained via the cable force – frequency calculation formula considering bending resistance and sag. The maximum error of cable force measurement is less than 1%, which meets the requirement of measurement accuracy. In order to eliminate the influence of temperature change on cable force, the two test times are both in the early morning of late August.

The comparison between the dead load cable force test result in 2006 and 2018 is shown in Fig. 6a. In the figure, cable force reduction is expressed by a negative number, whereas cable force increase is expressed by a positive number. The distribution trend of the measured dead load cable force in 2018 is basically consistent with that in 2006. A comparison of the two dead load cable forces indicates that the variation in cable force  $\Delta T$  is within 109.152 kN, and the change range is  $-2.41 \div 1.29\%$ . The number of stay cables with reduced force accounts for 83%,



Fig. 5. Test system for cable force

and substantial redistribution of internal force occurs. Cable force adjustment and cable force optimisation are suggested. There are many possible causes for the change in cable forces, based on the jammed and deformed expansion joint spotted during appearance inspection, one of the reasons is that the bridge at high latitude. With an annual temperature difference of up to 50°C, the bridge deck cannot expand and contract normally. Besides, the internal forces of cables must have changed with heavy vehicles. The second reason is that the cable force becomes smaller due to the relaxation of the stayed cables in the long-term operation [13]. The third reason is that the shrinkage and creep effect of concrete will lead to the reduction and redistribution of cable force as the cable-stayed bridge is a high-order statically indeterminate structure [14]. The ratio of the measured force under the self-weight to breaking force was defined as bearing ratio of ropes is shown in Fig. 6b. In the two tests in 2006 and 2018, the bearing ratio of the stay cable did not change significantly. The maximum load-bearing ratio at the shortest cable is 0.43, indicating that the strength reserve of the single cable itself is still high.

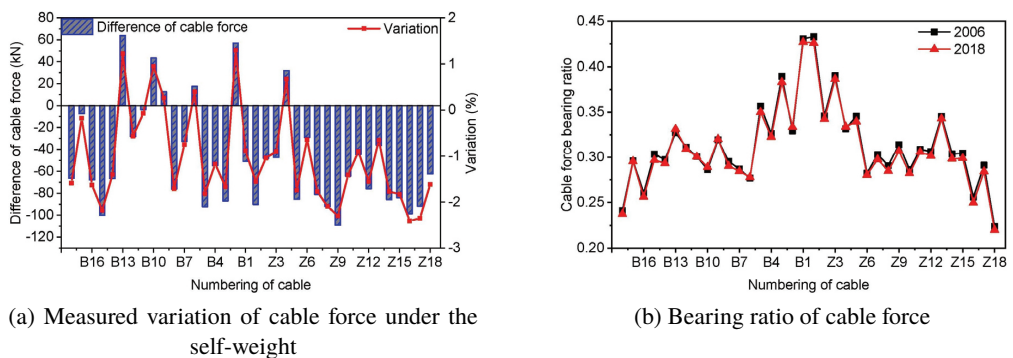


Fig. 6. Measured result for cable force

### 3.2. Dead load test of elevation of the bridge floor

The longitudinal displacement of the girder and the displacement of the bridge piers and abutments can be observed through an elevation test of the bridge floor. In this paper, the known benchmarks are retested and calibrated firstly, then the elevation points on the bridge floor are

surveyed. The selection of elevation measuring points on the bridge floor in 2018 is the same as that in 2006 to make the data comparative. The layout of the elevation measuring points on the bridge floor is shown in Fig. 7.

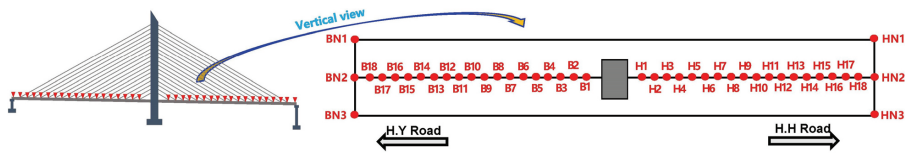
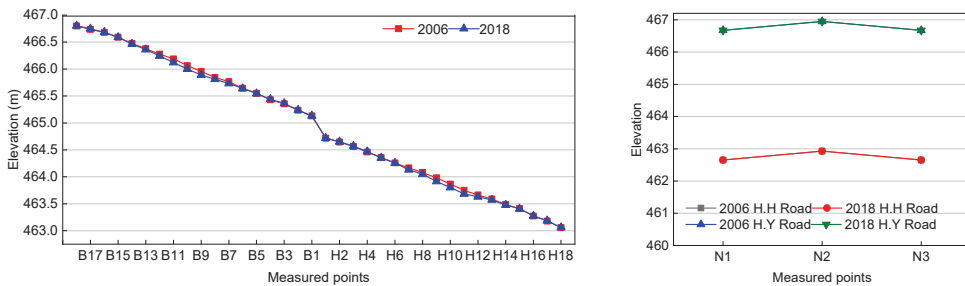


Fig. 7. Layout of the elevation measuring points on the bridge floor

The Elevation test result on the bridge floor are shown in Fig. 8. No difference in the transverse alignment at the pivot point of H.H Road and H.Y Road was found in 2018 and 2006. No uneven settlement occurred in the piers of the cable-stayed bridge. The longitudinal alignment indicates that the general variation and distribution trend of elevation in 2018 is basically the same as that in 2006. However, the dead load shows a downward deflection in the middle of the east–west span. Comparing the two measurement results between 2006 and 2018, the elevation of the east span bridge deck in 2018 is 66.7 mm lower than that in 2006 to the maximum, and that of the west span bridge deck is 67.2 mm lower than that in 2006 to the maximum. The reasons for this elevation change include redistribution of stayed cable force, shrinkage and creep of concrete in the 12 years period, and possible damage and deformation of the main girder. The degree of damage and deformation is further verified by static and dynamic load tests.



(a) Longitudinal alignment of the entire bridge

(b) Bearing ratio of cable force

Fig. 8. Transverse alignment at the pivot point

## 4. Static and dynamic test

### 4.1. Working conditions for static load test and layout of measuring points

The static load test for testing the mechanical performance of positive and negative bending moments on the most unfavourable section is divided into medium and unbalanced load. During and after loading, the displacement of the main girder and tower, the stress of the control section

and the key cable forces near the loading area are tested. The selection of the test conditions and the measuring points in 2018 is the same as that in 2006 to make the data comparative. The general layout of the static test section is shown in Fig. 9. The test conditions and loading positions are shown in Table 1.

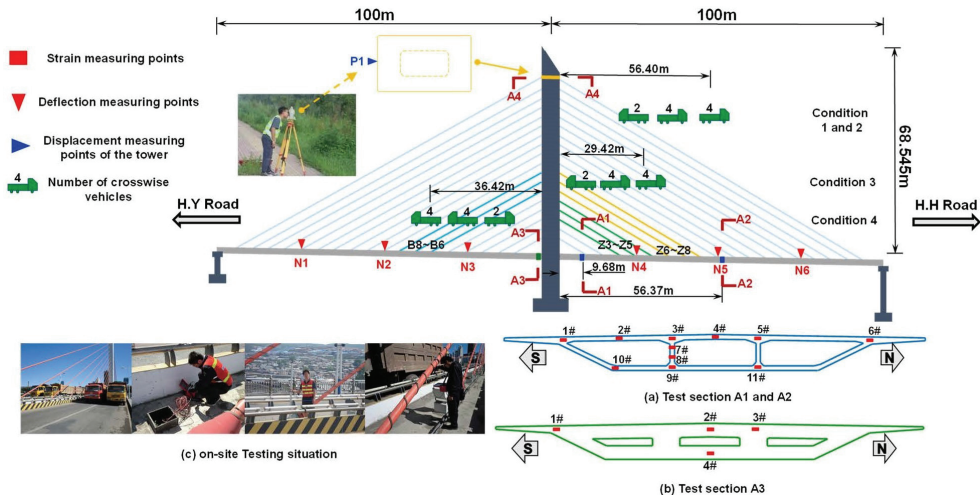


Fig. 9. General layout of the static load test section

Table 1. Working conditions for the test and loading positions

Conditions	Contents and positions
1	Section A2, symmetrical loading of maximum positive bending moment of the main girder on the side of H.H Road, 56.37 m from the axis of the main tower
2	Section A2, eccentric loading of maximum positive bending moment of the main girder on the side of H.H Road, 56.37 m from the axis of the main tower
3	Section A1, symmetrical loading of maximum negative bending moment of the main girder on the side of H.H Road, 9.68 m from the axis of the main tower
4	Section A3, symmetrical loading of maximum negative bending moment of the main girder at the root of the main tower on the side of H.Y Road

The test efficiency of two previous load tests is listed in Table 2. The load efficiency of 0.81 obtained from the test method for long-span concrete bridges in 2006 cannot meet the requirement of the ‘Code for the load test of roads and bridges’, that is, the minimum load efficiency is 0.95 because of the update in the experimental guidance [15]. The loading position in the 2006 experiment is retained in the 2018 experiment. However, the loaded vehicle weight is adjusted to meet the requirements of load efficiency. It can be seen from Table 1 that for Condition 1 and Condition 2 the load efficiency in 2018 is 25.9% higher than that of 2006. For Condition 3 and Condition 4, the load efficiency of 2018 is roughly the same as that of 2006.

Table 2. Working conditions for static load test and test efficiency

Static load conditions	Contents	Load efficiency in 2006	Load efficiency in 2018
1	Section A2 is symmetrically loaded by the maximum positive bending moment.	0.81	1.02
2	Section A2 is eccentrically loaded by the maximum positive bending moment.	0.81	1.02
3	Section A1 is symmetrically loaded by the maximum negative bending moment.	1.00	0.98
4	Section A3 is symmetrically loaded by the maximum negative bending moment.	1.02	1.01

## 4.2. Strain test result and analysis

The maximum strains of the top and bottom of the concrete beam under the action of step loading tested in 2006 and 2018 are listed. The measured strains were obtained by the general-purpose tester with strain gauge made by KINGMACH. If the strain is tensile, then it is positive; if it is pressure, then it is negative (Table 3). Under loading condition 1, the measured strain at 4# measuring point of section A2 in 2018 is increased by 13  $\mu\epsilon$ , or 21.0%, compared with that in 2006; the measured strain at 9# measuring point of section A2 in 2018 is increased by 9  $\mu\epsilon$ , or 7.0%, compared with that in 2016. Under Condition 2, the measured strain at 4# measuring point of section A2 in 2018 is increased by 12  $\mu\epsilon$ , or 17.4%, compared with that in 2006; the measured strain at 9# measuring point of section A2 in 2018 is increased by 4  $\mu\epsilon$ , or 2.9%, compared with that in 2006. Under Condition 3 and 4, the measured top and bottom strains in 2018 and 2006 are roughly the same, but under Condition 4, the ratio of measured strain to the calculated strain of top and bottom of A3 section in 2006 and 2018 is both 0.98,

Table 3. Comparison of the maximum strain measuring points in all sections

Test conditions and section	Positions of measuring points	Calculated strain / $\mu\epsilon$		Measured strain / $\mu\epsilon$		Measured strain/ calculation strain	
		2006	2018	2006	2018	2006	2018
Condition 1 Section A2	Top 4# measuring point	-164	-187	-62	-75	0.38	0.40
	Bottom 9# measuring point	241	263	128	137	0.53	0.52
Condition 2 Section A2	Top 4# measuring point	-182	-207	-69	-81	0.38	0.39
	Bottom 9# measuring point	270	289	138	142	0.51	0.49
Condition 3 Section A1	Top 4# measuring point	62	60	29	27	0.47	0.45
	Bottom 9# measuring point	-94	-91	-30	-28	0.32	0.31
Condition 4 Section A3	Top 2# measuring point	46	-	45	-	0.98	-
	Bottom 4# measuring point	-80	-78	-78	-76	0.98	0.98

which indicates that the safety stock of the section is low. Under Condition 1–4, the ratio of measured strain to calculated strain in 2018 and 2006 is roughly the same, which indicates that the main girder of the bridge has no structural damage during 12 years of operation. The increased measured strain in 2018 than that in 2016 is mainly caused by the increase in load efficiency.

### 4.3. Deflection test result and analysis

The measured and calculated values of the deflection in the longitudinal direction along the main girder under the action of vehicle load in the two tests are listed in Fig. 10. The measured deflections were obtained by the level with rulers. Under loading condition 1, the measured deflection of the loading section in 2018 is 6.7 mm, or 12.1%, larger than that in 2016. Under Condition 2, the measured deflection of the loading section in 2018 is 6.7 mm, or 12.1%, larger than that in 2016. In Condition 3 and 4, the deflection of the loading section in 2018 is roughly the same as that in 2006. The increase in measured deflection in 2018 is mainly caused by the increase in load efficiency. Under Condition 1–4, the ratio of measured deflection to calculated deflection in 2018 and 2006 is roughly the same, which indicates a good structural stiffness of the bridge after 12 years of operation.

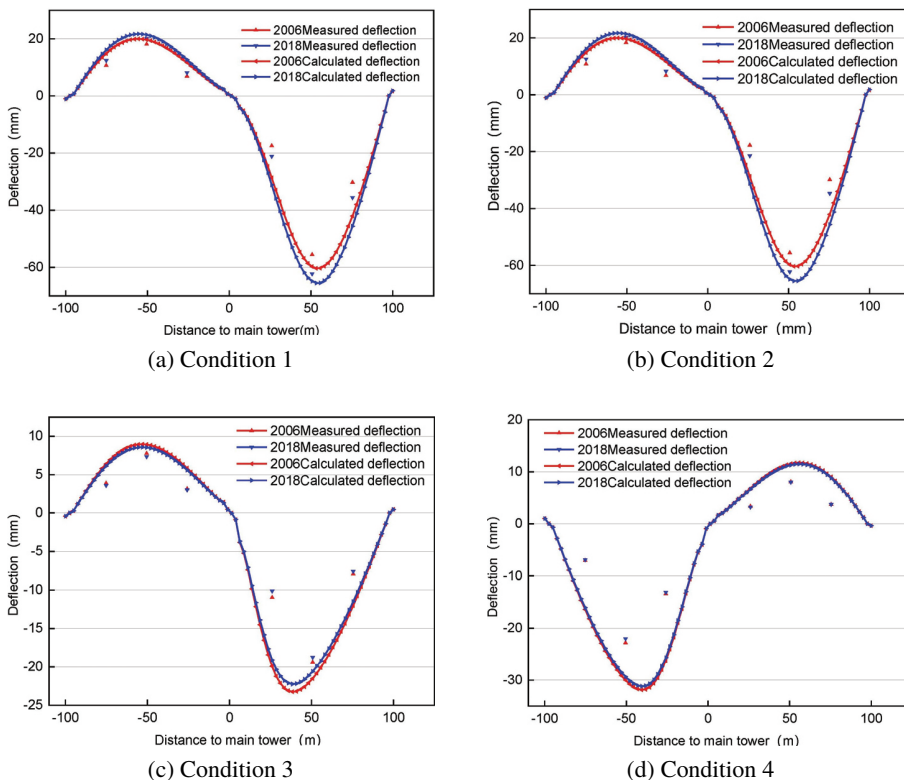


Fig. 10. Measured and calculated deflection values in measuring points under different loading conditions

#### 4.4. Test results and analysis of the main tower deviation

The calculated values and measured values of the main tower deviation in the top section (A4) under the action of step loading as tested in 2006 and 2018 are shown in Fig. 11. The measured values were obtained by the total station shown in Fig. 9. If the bridge tower leans to the side of H.H Road, then it is positive.

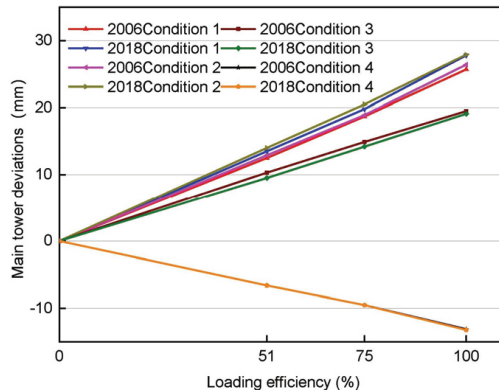


Fig. 11. Relationship between the displacement increment at the main tower top and load increment

Fig. 11 depicts that, under loading condition 1, the measured deviation of the main tower in 2018 is 2.1 mm larger than that in 2006. Under Condition 2, the measured deviation of the main tower in 2018 is 1.5 mm larger than that in 2006. Under Condition 3, the measured deviation of the main tower in 2018 is 0.4 mm larger than that in 2006. Under Condition 4, the measured deviation of the main tower in 2018 is 0.4 mm larger than that in 2006. The ratio of measured deviation to calculated deviation in 2018 is higher than that in 2006, with an increase of  $2.7 \div 3.5\%$ , indicating that the structural safety stock of the bridge has decreased after 12 years of operation. The analysis shows that the reason for the above ration increase is the reduction and redistribution of stayed cable force.

#### 4.5. Test results and analysis of stay cable force increment

The incremental values of key stay cable force under the test load of different conditions during the 2006 and 2018 experiments are tested. The tested values are compared with the corresponding calculated values. The test results are shown in Table 4.

Table 4 shows that the measured values of cable force increment in 2006 and 2018 are less than the calculated values. The ratios of measured increment to the calculated cable force increment are in the range of  $0.49 \div 0.87$  and  $0.50 \div 0.92$ , respectively, which do not exceed the upper limit of the specification of 1.00. The changing trends of cable increments under test conditions 1–3 in the two tests are consistent with the theoretical values. In addition, the cable force increment decreases gradually from short cable to long cable. In the same test section, the cable force increment decreases faster under eccentric loading than under symmetrical loading. The fatigue loads on the stay cables in the two tests are live loads with a stress

Table 4. Comparison of changing values of stay cable force under different test conditions

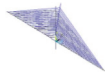
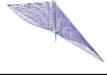
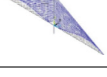
Test conditions	Number of tested cables	Calculated cable force increment/ kN		Measured cable force increment/ kN		Measured cable force increment/ calculated cable force increment		Measured cable force increment/ Ultimate tensile cable force	
		2006	2018	2006	2018	2006	2018	2006	2018
1	z6	749	884	641.9	751.4	0.86	0.85	0.05	0.06
	z7	696	842	578.4	707.3	0.83	0.84	0.04	0.05
	z8	665	792	534.9	641.5	0.80	0.81	0.04	0.05
2	z6	827	974	650.8	847.4	0.87	0.87	0.05	0.07
	z7	752	936	486.0	673.9	0.70	0.72	0.04	0.06
	z8	704	867	403.7	537.5	0.61	0.62	0.03	0.04
3	z3	473	462	412.4	406.6	0.87	0.88	0.03	0.03
	z4	442	439	271.1	263.4	0.61	0.60	0.02	0.02
	z5	427	430	207.9	215.0	0.49	0.50	0.02	0.02
4	B3	528	519	358.8	352.9	0.68	0.68	0.03	0.03
	B4	534	526	369.7	483.9	0.69	0.92	0.03	0.04
	B5	555	545	380.1	372.5	0.68	0.68	0.03	0.03

amplitude below 0.07. The fatigue load on the cable-stayed bridge hardly reaches the most unfavourable load. The fatigue effect is small, and the structural safety is unaffected. B4# cable force increment under condition 4 in the test of 2018 is 483.9 MPa, which is abnormally larger than 369.7 MPa. Therefore, the ratio of the measured increment to the calculated increment is 0.92. This condition does not affect the structural safety. However, the changing trend is related to the redistribution of cable force. This study therefore suggests adjusting and optimising the cable force.

#### 4.6. Ambient vibration

Under the condition that the test environment is basically the same, the first three-order theoretical and test frequencies of the cable-stayed bridge measured in 2006 and 2018 are listed in Table 5. The measured frequency of the two tests is higher than the theoretical frequency, which shows that the cable-stayed bridge has sufficient rigidity and good dynamic performance in the operation stage. The measured second and third-order frequencies of the cable-stayed bridge in 2018 are smaller than the measured values in 2006. Thus, the longitudinal bending stiffness of the girder has declined after 12 years of operation. The reason is the reduction and redistribution of stayed cable force.

Table 5. Test result for ambient vibration

Order	Frequency/ Hz			Vibration mode
	Theoretical value	Measured value in 2006	Measured value in 2018	
1	0.53	0.61	0.62	
2	0.68	0.72	0.71	
3	0.99	1.05	1.04	

## 5. Conclusion

The Suifenhe cable-stayed bridge in China is regarded as the study object. We tested this level-pivot hinged swiveled construction of cable-stayed bridge, which has been in operation for 12 years, two times. Combined with an ansys finite element model, the comparison between the theoretical and measured data and the comparison amongst measured data are analysed. The following conclusions are obtained:

1. Comparing the two dead load cable forces between 2018 and 2006, change varies from  $-2.41\%$  to  $1.29\%$ , the overall cable force has significant internal force redistribution. It is suggested that the cables of the cable-stayed bridge be adjusted to optimize the cable force. The elevation of the bridge deck at the support in 2018 is roughly the same as that in 2006, which indicates that there is no uneven settlement of the piers of the cable-stayed bridge. In 2018, the elevation of the bridge deck is 67.2 mm lower than that in 2006 to the maximum, which is mainly caused by the shrinkage and creep of concrete in 12 years.
2. The ratio of the measured value to the theoretical value of strain, main girder deflection, main tower deflection, and cable force increase are all less than 1.00 for static load tests in 2018 and in 2006, which indicates that a good operational performance of bridge structure. The comparison between the two static load test results shows that the ratio of the measured deflection of the main tower to the theoretical value in 2018 is increased by  $2.7\div 3.5\%$  compared with that in 2006, and the increase of the B4# cable force, 483.9 MPa, under condition 4 in 2018 test is significantly larger than that in 2006, indicating that the reduction and redistribution of the stayed cable force will have adverse effects on the safety of the bridge structure after long-term operation.
3. In the ambient vibration test, the measured frequencies in the two tests are larger than the theoretical ones. This difference shows that the cable-stayed bridge has sufficient rigidity and good dynamic performance. The second- and third-order frequencies measured in 2018 are smaller than the measured values in 2006. The longitudinal bending frequency of the girder of the cable-stayed bridge after 12 years of operation has declined, indicating a reduction and redistribution of cable forces.
4. According to the results of two static and dynamic load tests in 2018 and 2006, the main problems of the Suifenhe cable-stayed bridge after 12 years of operation are cable force

loss and cable force redistribution. It is suggested that the cable force to be readjusted and tested regularly in the future.

Static and dynamic tests shall be carried out for cable-stayed bridges that have been in operation for more than 10 years to check the changes of strain and deflection of the bridge, and cables shall be adjusted promptly to optimize the operation state of cable-stayed bridges.

## Acknowledgments

This work was supported by the Research on the mechanical characteristics of steel box girders in cold regions (Department of Transportation of Heilongjiang Province, China, Grant No. 2020HLJ018).

## References

- [1] J. Zhang, Q. Zhong, "The achievement and development of bridge construction by level-pivot swivel method". *Railway Standard Design*, no. 6, pp. 19–28, 1992, DOI: [10.13238/j.issn.1004-2954.1992.06.003](https://doi.org/10.13238/j.issn.1004-2954.1992.06.003).
- [2] W. Wang, "Swivel construction of rigid cable-stayed bridge on Daliying Railway". *Bridge Construction*, no. 02, pp. 31–34, 1998.
- [3] S. Mao, "Wivel construction technology of the cable-stayed bridge across Shitai Railway on Shitai Highway". *Journal of Railway Engineering Society*, no. 1, pp. 58–62, 2009, DOI: [10.3969/j.issn.1006-2106.2009.01.013](https://doi.org/10.3969/j.issn.1006-2106.2009.01.013).
- [4] Y. Guo, H. Li, "Stress analysis of swivel structure of Zhoucheng cable-stayed bridge". *Journal of China and Foreign Highway*, vol. 33, no. 1, pp. 119–122, 2013, DOI: [10.14048/j.issn.1671-2579.2013.01.055](https://doi.org/10.14048/j.issn.1671-2579.2013.01.055).
- [5] Y. Niu., H. Li., W. Quan., L. Zhang, "Study on level-pivot hinge of super large tonnage cable-stayed bridge". *Journal of Railway Engineering Society*, vol. 32, no. 06, pp. 34–39+56, 2015, DOI: [10.3969/j.issn.1006-2106.2015.06.008](https://doi.org/10.3969/j.issn.1006-2106.2015.06.008).
- [6] J. Hu, "Study on deformation and stress state of NXZT asymmetric single tower swivel cable-stayed bridge". Master thesis, Central South University, China, 2014.
- [7] N. Fuchs, K. Tomlinson, and R. Buckby, "El Ferdan Bridge, Egypt: the world's longest swing bridge". *Proceedings of the Institution of Civil Engineers*, vol. 156, no. 1, pp. 21–30, 2003, DOI: [10.1680/bren.2003.156.1.21](https://doi.org/10.1680/bren.2003.156.1.21).
- [8] L. Lv, Y. Jia, and Y. Ji, "Evaluation on bearing capacity of cable-stayed bridge with two towers based on load test". *Journal of Architecture and Civil Engineering*, vol. 36, no. 3, pp. 101–109, 2019.
- [9] S. Cao, Z. Tian, and J. Zhao, "Load test of Malinghe Bridge". *Journal of China and Foreign Highway*, vol. 32, no. 5, pp. 160–163, 2012, DOI: [10.14048/j.issn.1671-2579.2012.05.021](https://doi.org/10.14048/j.issn.1671-2579.2012.05.021).
- [10] W. Wang, "Study on mechanical properties of partial cable-stayed bridges with composite girder with corrugated steel webs". Master thesis, Southeast University, China, 2018.
- [11] F. Cao, L. Yu, and Q. Zhai, "Study on the influence factors of measuring cable force of cable-stayed bridge by vibration frequency method". *Railway Engineering*, no. 5, pp. 27–30, 2017, DOI: [10.3969/j.issn.1003-1995.2017.05.08](https://doi.org/10.3969/j.issn.1003-1995.2017.05.08).
- [12] C. Elsa and C. Álvaro, "Dynamic testing of cable structures". *MATEC Web of Conferences*, vol. 24, 2015, DOI: [10.1051/mateconf/20152401002](https://doi.org/10.1051/mateconf/20152401002).
- [13] Y. Bao, B. Jiang, and W. Li, "Parameter Sensitivity Analysis of extradosed bridge in Operation Stage". *Journal of China and Foreign Highway*, vol. 65, no. 8, pp. 216–222, 2020.
- [14] A. Guo, "Research on influence and control measures of shrinkage and creep on long-span railway prestressed concrete cable-stayed bridge". *Railway Standard Design*, vol. 65, no. 6, pp. 73–77, 2021, DOI: [10.13238/j.issn.1004-2954.202006010006](https://doi.org/10.13238/j.issn.1004-2954.202006010006).
- [15] Chinese National Standards. JTG/T J21-01-2015: Load Test Methods for Highway Bridge, Beijing, China, 2015.